Progress and prospects of atmospheric environmental sciences in China

Fahe Chai, Abdelwahid Mellouki, Yujing Mu, Jianmin Chen, Huiwang Gao, Hong Li

CONTENTS

Special Issue: Progress and prospects of atmospheric environmental sciences in China

Mechanism and kinetics study on the ozonolysis reaction of 2,3,7,8-TCDD in the atmosphere

Jing Bai[1], Xiaomin Sun[1,*], Chenxi Zhang[1], Chen Gong[1], Jingtian Hu[1], Jianghua Zhang[2]

1. Environment Research Institute, Shandong University, Jinan 250100, China

2. School of Management, Shandong University, Jinan 250100, China

A B S T R A C T

The ozonolysis of 2,3,7,8-tetra-chlorodibenzo-p-dioxin (2,3,7,8-TCDD) is an efficient degradation way in the atmosphere. The ozonolysis process and possible reactions path of Criegee Intermediates with NO and H_2O are introduced in detail at the method of MPWB1K/6-31+G(d,p)//MPWB1K/6-311+G(3df,2p) level. In ozonolysis, H_2O is an important source of OH radical formation and initiated the subsequent degradation reaction. The Rice-Ramsperger-Kassel-Marcus (RRKM) theory was applied to calculate rate constants with the temperature ranging from 200 to 600 K. The rate constant of reaction between 2,3,7,8-TCDD and O_3 is 4.80×10^{-20} cm^3/(mole·sec) at 298 K and 760 Torr. The atmospheric lifetime of the reaction species was estimated according to rate constants, which is helpful for the atmospheric model study on the degradation and risk assessment of dioxin.

Introduction

With the increasing of environmental awareness, the persistent organic pollutants (POPs) have leaped into people's view. As typical POPs, dioxins with the carcinogenic, teratogenic, and mutagenic effects (Schecter, 1994), are a class of structurally and chemically related polyhalogenated aromatic hydrocarbons that mainly include polychlorinated dibenzo-p-dioxins (PCDDs) and dibenzofurans (PCDFs) (Schecter et al., 2006; Kulkarni et al., 2008). PCDD/Fs are mainly emitted to the atmosphere from incineration, combustion, industrial and reservoir sources (Lin et al., 2008; Chiu et al., 2011). Chi et al. (2007, 2009) studied the historical trends of PCDD/Fs in sediments buried in a reservoir and measured atmospheric deposition by automated and traditional samplers in Northern Taiwan. Because of their biological

effects and high toxicities, the investigation of dioxin's destruction is of great significance. To destroy these recalcitrant compounds, a growing interest has been provoked in developing efficient and economically feasible remediation technologies including incineration and thermal treatment (Weber et al., 1999; Lundin and Marklund, 2005), catalytic destruction (Ide et al., 1996; Debecker et al., 2011), photocatalysis (Choi et al., 2000), photolysis (Konstantinov et al., 2000; Rayne et al., 2002; Choi et al., 2004), radiolysis (Hilarides et al., 1994), ozonolysis (Vollmuth and Niessner, 1995) and biodegradation (Mori and Kondo, 2002; Fennell et al., 2004). However, most of these methods are not suitable for the degradation of PCDD/Fs in the atmosphere. Gaseous PCDD/Fs are primarily depleted when reacting with OH, NO_3 radicals and O_3 in the atmosphere (Kwok and Atkinson, 1995; Atkinson, 1996). All of those oxidants play an important role in the atmospheric chemistry. The reaction of gaseous PCDD/Fs congener with OH is reported to be at least 8 and 3 orders of magnitude faster than their reactions with

* Corresponding author. E-mail: sxmwch@sdu.edu.cn

O_3 and NO_3 radicals (Atkinson, 1996). And the OH and O_3 concentration in atmosphere are 2.0×10^6 mole/cm^3 and 7.0×10^{11} mole/cm^3, respectively. Obviously the O_3 concentration is much higher than OH radical, thus the role of ozone can not be ignored in atmospheric environment. Furthermore, the main oxidants in the atmosphere are OH radical and O_3 during the daytime, while the main oxidants are NO_3 and O_3 at night. So the ozone takes effect all the time and it is a highly reactive gas with a strong oxidability, which can promote heterogeneous chemical reactions faster with the organic matters, especially those with double bonds in their chemical systems. Recently the investigation of O_3 has aroused considerable attention (José et al., 2005; Al-Alawi et al., 2008), and many experimental and theoretical studies of the ozonolysis reactions have been carried out. Most importantly, the ozone arises from a variety of resources, including anthropogenic sources and natural sources. Given that dioxin congeners share similar chemical and physical properties, 2,3,7,8-TCDD, the most toxic congener among all dioxin congeners (Schecter et al., 2006; Kulkarni et al., 2008), is selected as a typical one in this study.

Although the experiments of PCDD/Fs' ozonolysis have been performed, the reaction mechanism is still not clear. Recently, ab initio molecular orbital calculation is widely adopted to interpret experimental findings and to provide theoretical understanding for chemical transformation processes. Many theoretical studies on the formation of PCDD have been reported (León et al., 2002; Khachatryan et al., 2003; Fabian and Janoschek 2006; Altarawneh et al., 2007, 2008; Zhang et al., 2008, 2010; Qu et al., 2009; Xu et al., 2010, 2011; Yu et al., 2011). Therefore, invalidation of the degradation mechanism under different conditions is necessary. Zhang et al. (2011, 2012) used quantum chemical theory to clarify the mechanism for OH-initiated degradation of 2,3,7,8-TCDD and 2,3,7,8-TCDF in the presence of O_2 and NO/H$_2$O. Wen et al. (2010) reported a possible ozonolysis degradation mechanism of the 2,3,7,8-TCDD. But it can be found that Wen's research is only based on the stereoeffect, while the electronic effect is neglected. By means of thermodynamic and kinetic analysis, the two easiest pathways of the ozonolysis degradation over the low temperature range are given in this article. Some reactions of intermediates with NO and H$_2$O are also discussed. The rate constants are calculated and the atmospheric lifetime of the reaction species is estimated accordingly.

1 Computational method

1.1 Geometry optimization

The unrestricted MPWB1K method is used to treat systems with an even number of electrons but with partial open-shell character, such as ozone, the Criegee biradicals. The MPWB1K method is a hybrid density functional theory model with excellent performance for thermochemistry, thermochemical kinetics, hydrogen bonding, and weak interactions. It is well-known that MPWB1K is an excellent method to predict transition state geometries and thermochemical kinetics, based on the modified Perdew and Wang exchange functional (MPW) and Becke's 1995 correlation functional (B95) (Zhao and Truhlar, 2004). MPWB1K method has ever been applied to the study of ozonolysis reactions (Yang et al., 2007, 2008). In all reaction channels, the geometry structures of various reactants, transition states, intermediates and products are optimized at the MPWB1K/6-31+G(d,p) level. The vibrational frequencies are also calculated at the same level to determine the nature of stationary points. The selection of basis set is important to get precise results (Zhang et al., 2000). The single-point energy calculations are performed at a higher level of theory MPWB1K/6-311+G(3df,2p). All the work is performed using the Gaussian 03 programs (Frisch et al., 2003) and SGI workstation.

1.2 Kinetic calculation

The initial information obtained from ab initio calculations allows us to calculate the rate constants. The kinetic calculations have been carried out using Rice-Ramsperger-Kassel-Marcus (RRKM) theory modified by Hou and Wang (2007). This method has been successfully used in the previous ozonolysis study (Wang et al., 2010; Sun et al., 2011).

2 Results and discussion

2.1 Ozonolysis reaction

Scheme 1 shows the structure of 2,3,7,8-TCDD. There are four different kinds of C=C double bonds labeled as A, B, C and D, respectively, which can be attacked by O_3. According to the stereoeffect, Wen et al. (2010) has reported that the D position is the most probable pathway for 2,3,7,8-TCDD to react with O_3. In fact, both the electronic effect and stereoeffect should be taken into consideration. The thermodynamic and kinetic calculations of the four positions with O_3 are performed. The potential energy surface is drawn in **Fig. 1**. Obviously, the barriers of path A (10.29 kcal/mol) and path B (9.79 kcal/mol) are lower than those of path C (14.51 kcal/mol) and path D (14.93 kcal/mol). Due to the distinction of calculation methods, the potential barrier of path D is different from the data (12.25 kcal/mol) of Wen et al. (2010).

The ozonolysis reaction is initiated by addition of ozone to the double bonds of 2,3,7,8-TCDD to produce a primary ozonide. The unstable five-membered ring of primary ozonide can easily break up in the the C–C bond and O–O

bonds part to generate a high-energy criegee intermediate and a relatively stable aldehyde or ketone. In this article, the four ozonolysis reactions are similar, but path A and B are chosen to discuss the mechanism since they take up the major proportion in most of the temperature range. The structures of all the reactants, intermediates, transition states and products are listed in **Fig. S3**.

2.1.1 Reaction channel A

The main possible reaction paths for the reaction of 2,3,7,8-TCDD with O_3 are listed in **Scheme 2**. Reaction channel A is the O_3 addition to the $> C2 = C3 <$ bond. Firstly, 2,3,7,8-TCDD reacts with O_3 via TSa1 to generate IMa1, with a potential barrier of 10.29 kcal/mol and the reaction heat of −36.80 kcal/mol. Then the C2–C3 and O1–O3 bonds of the five-membered ring in the IMa1 will be broken via TSa2 to form IMa2, the barrier is 25.30 kcal/mol and the reaction heat is −11.00 kcal/mol (**Fig. 2**). It can be seen that the IMa2 contains a benzene ring and two C=C double bonds. Obviously, the ozone can be added to the benzene ring or the C=C double bonds sequentially. With their barriers compared, the reaction IMa2 + O_3 → TSa32 → IMa32 is determined to be the most probable
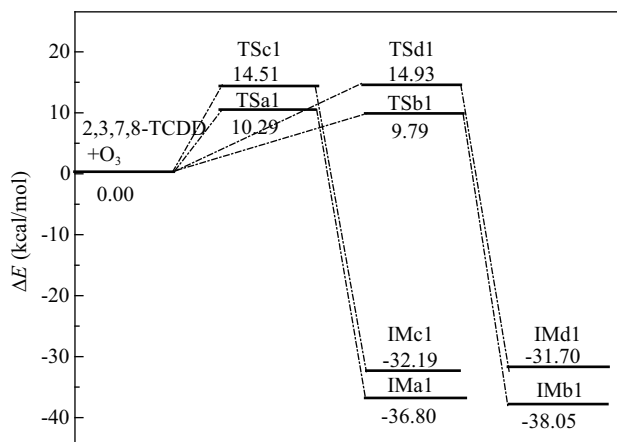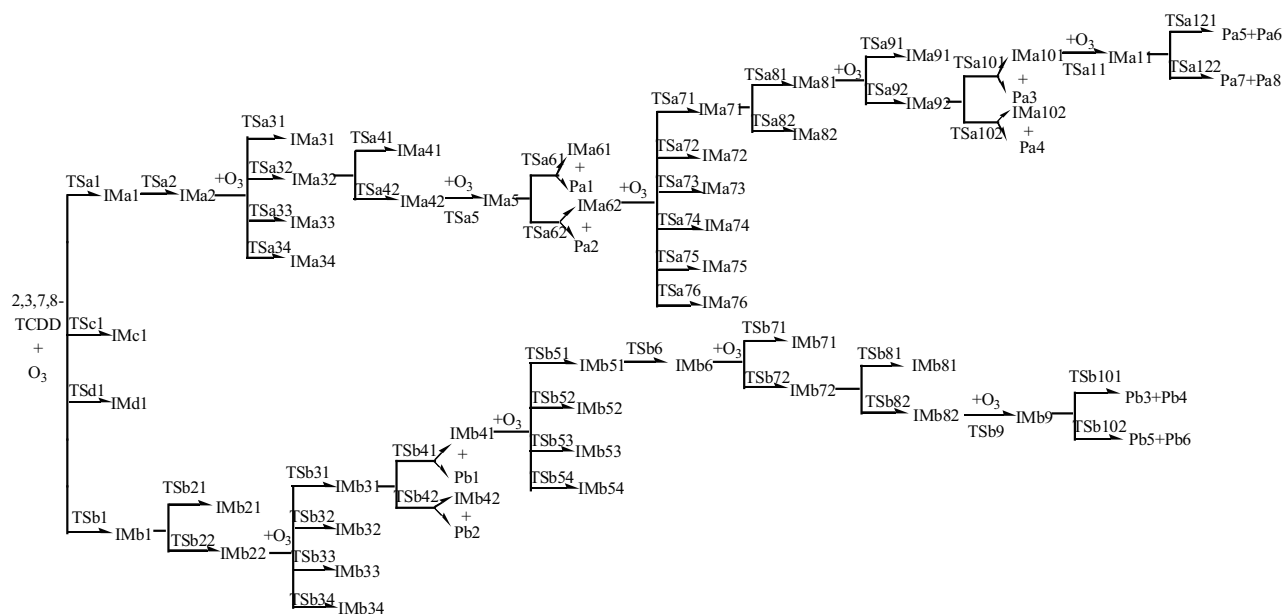

Fig. 1 Profile of potential energy ΔE surface for the first step reaction of 2,3,7,8-TCDD with O_3.

reaction channel. The subsequent ozonolysis processes are similar to the above discussed and the whole reaction route is listed in the **Scheme 1** and the profile of potential energy surface for the subsequent reactions of reaction channel A is drawn in **Fig. S1**.

2.1.2 Reaction channel B

The reaction channel B is the O_3 addition to the $> C1 = C2 <$ which has the lowest potential barrier among the four channels. Firstly, the 2,3,7,8-TCDD reacts with O_3 to produce IMb1 via TSb1 with a potential barrier of 9.79 kcal/mol and a relative energy of −38.05 kcal/mol (**Fig. 1**). The asymmetric IMb1 is different from the symmetrical IMa1, so that the five-membered ring in IMb1 has two pathways to break and generate two intermediates, that is, IMb21 and IMb22, respectively. Similarly, IMb22 is chosen as the reactant in the subsequent reaction after
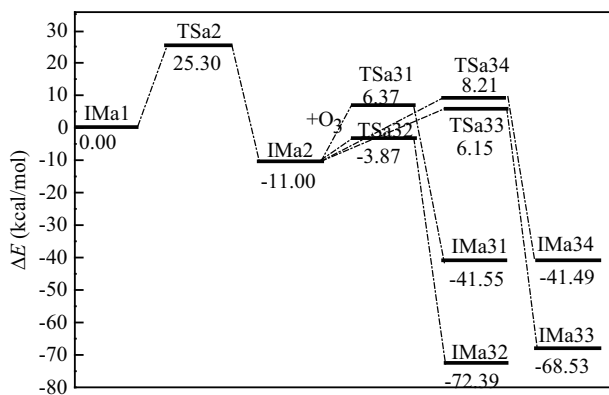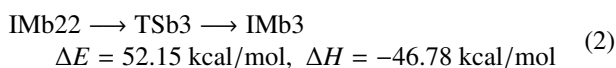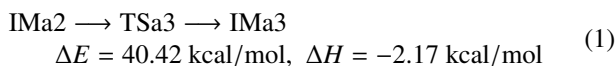

Scheme 1 Structure of 2,3,7,8-TCDD.

Scheme 2 Main possible reaction paths for the reaction of 2,3,7,8-TCDD with O_3.

Fig. 2   Profile of potential energy surface for the IMa1 and the following reactions.

the potential barrier and relative energy are compared (**Fig. 3**). The ozonolysis reaction occurs unceasingly until the products do not contain double bonds any longer. The profile of potential energy surface for the subsequent reactions of reaction channel B is drawn in **Fig. S2**.

The ozonolysis reaction initiated by C or D position is similar to the reaction channel A and B discussed above.

According to many reported results, the unimolecular reactions such as isomerization are also very important. Consideration of the large system of reactants, the IMa2 and IMb22 are only chosen to study the mechanism of isomerization. The reaction path is described as follows:

$$IMa2 \longrightarrow TSa3 \longrightarrow IMa3$$
$$\Delta E = 40.42 \text{ kcal/mol}, \quad \Delta H = -2.17 \text{ kcal/mol} \quad (1)$$

$$IMb22 \longrightarrow TSb3 \longrightarrow IMb3$$
$$\Delta E = 52.15 \text{ kcal/mol}, \quad \Delta H = -46.78 \text{ kcal/mol} \quad (2)$$

From the values of reaction barrier, a conclusion can be drawn that the isomerization reactions are not easy to occur to intermediates which contain the benzene ring.
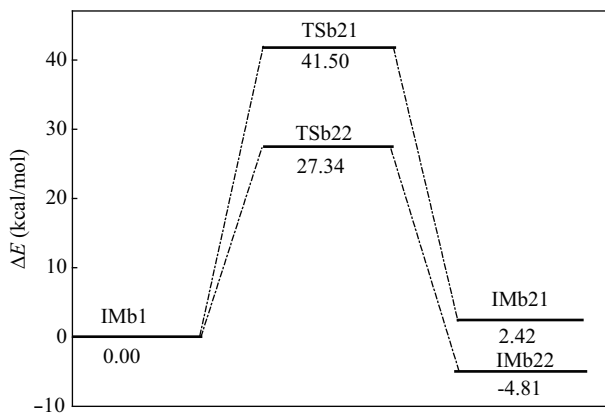

Fig. 3   Profile of potential energy surface for the IMb1.

2.2 Reactions in the presence of NO and H₂O

It should be pointed out that the ozonolysis reactions of 2,3,7,8-TCDD discussed above will occur only on the existence of ozone. It is well known that there are many abundant atmospheric precusors in the atmosphere, such as NO and H_2O. The criegee intermediates produced from the reaction of ozonolysis of 2,3,7,8-TCDD can react easily with these precursors. Some criegee intermediates in reaction channel A and B will be chosen as research object to discuss the reaction mechanism with NO and H_2O.

2.2.1 Reaction of IMa2

In the reaction channel A, the first criegee intermediate is IMa2. The profiles of the potential energy surface of IMa2 with NO and H_2O are drawn in **Fig. 4**. The potential barrier and exothermic energy for the process of IMa2 + NO → S31a → IM31a + NO_2 are 9.50 kcal/mol and 78.87 kcal/mol, respectively. This low barrier energy and high exothermic energy in this process mean that the O atom abstraction by NO can occur easily. So this process is both thermodynamically and kinetically favorable. IM31a is a kind of intermediates which contains group "$-\overset{\text{O}}{\underset{}{\text{C}}}-\text{o}-$" and is easy to hydrolyze.

Hasson et al. (2003) has studied the role of the water vapor in the alkene ozonolysis. It is pointed out that water vapor is an additional source of OH radicals in the reaction with criegee intermediates. The mechanism is proposed (**Fig. 5**) and the route R(1) is the most probable reaction channel.

IMa2 can react with H_2O to form a van der Waals complex IM3a, and then it will generate IM4a-OH via TS3a. In TS3a, the H atom of H_2O is transferred to the O atom of "C=O-O" and the OH group of H_2O approaches the C atom. The IM4a-OH will be decomposed quickly because it is a complex with rich energy. Then the OH radical will play a very important role in dioxin degradation. The energy barrier and exothermic energy of this process are 11.75 kcal/mol and 29.41 kcal/mol, respectively.
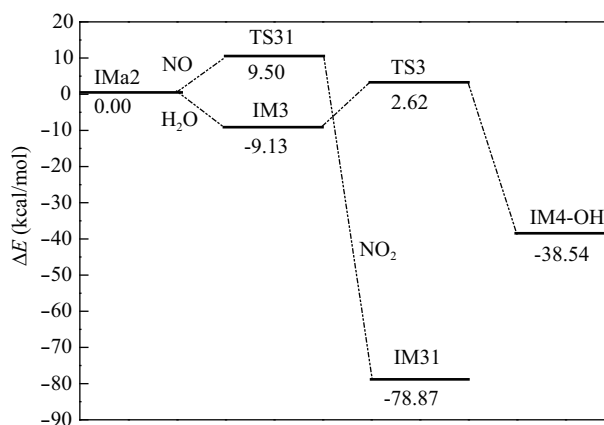

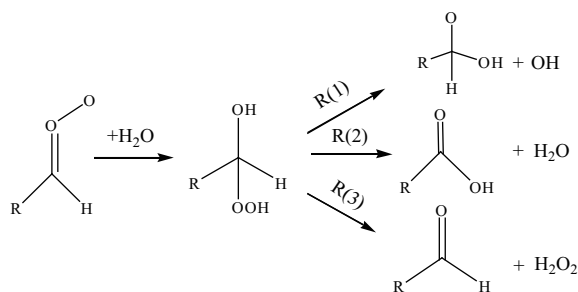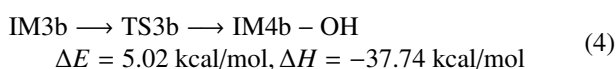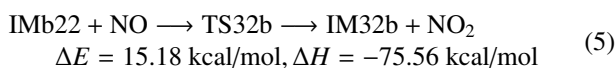**Fig. 4**   Profile of potential energy surface for the IMa2 react with NO and H_2O.

Fig. 5 Possible reactions of criegee intermediates with H_2O (Hasson et al., 2003).

2.2.2 Reacion of IMb21 and IMb22

In the ozonolysis reaction channel B, the criegee intermediates generated from the reactions are IMb21 and IMb22. IMb21 can react with H_2O which is the same as the reaction of IMa2 with H_2O. The profile of the potential surface is given as follows:

$$IMb21 + H_2O \longrightarrow IM3b \tag{3}$$
$$\Delta H = -9.26 \text{ kcal/mol}$$

$$IM3b \longrightarrow TS3b \longrightarrow IM4b - OH \tag{4}$$
$$\Delta E = 5.02 \text{ kcal/mol}, \Delta H = -37.74 \text{ kcal/mol}$$

While IMb22 can be abstracted by NO, which is similar to the reaction of IMa2 with NO.

$$IMb22 + NO \longrightarrow TS32b \longrightarrow IM32b + NO_2 \tag{5}$$
$$\Delta E = 15.18 \text{ kcal/mol}, \Delta H = -75.56 \text{ kcal/mol}$$

Here, the property of IM32b is similar to that of IM31a discussed previously. The other criegee intermediates produced in the ozonolysis reaction can also react with NO and H_2O, similar to the reaction of IMa2, IMb21 and IMb22.
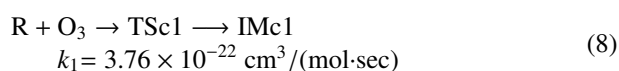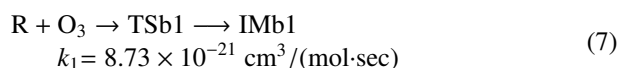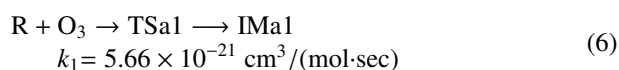
2.3 Rate constants and atmospheric lifetimes

So far, the whole degradation mechanism is discussed in detail. The rate constants for the reaction of PCDD/Fs with O_3 have been studied by many groups. Kwok et al. (1995) has reported the rate constant for the gas-phase reaction of debenzo-p-dioxin with O_3 at 297 ± 2 K and atmospheric pressure of air using a relative rate method. The rate constant is $< 5 \times 10^{-20}$ cm³ (mole·sec) which is consistent with expectations based on kinetic data for gas phase reactions of O_3 with other aromatic compounds.

In this study, the RRKM theory modified by Hou and Wang (2007) is used to calculate the rate constants. The generally accepted temperature ranges from –56 to 15°C in the troposphere. Flue gas temperatures of 240–260°C are generally needed for effective PCDD/Fs destruction in field tests. Then a wider range of 200–600 K is chosen to study the relationship between the temperature and rate constants.

There are no previous data for the reaction of 2,3,7,8-TCDD + O_3 → TS → IM. The rate constants of each channel are listed in **Table 1**. The rate constants at 298.15 K are taken as examples.

$$R + O_3 \rightarrow TSa1 \longrightarrow IMa1 \tag{6}$$
$$k_1 = 5.66 \times 10^{-21} \text{ cm}^3/(\text{mol·sec})$$

$$R + O_3 \rightarrow TSb1 \longrightarrow IMb1 \tag{7}$$
$$k_1 = 8.73 \times 10^{-21} \text{ cm}^3/(\text{mol·sec})$$

$$R + O_3 \rightarrow TSc1 \longrightarrow IMc1 \tag{8}$$
$$k_1 = 3.76 \times 10^{-22} \text{ cm}^3/(\text{mol·sec})$$

The total rate constant design formula of 2,3,7,8-TCDD with O_3 is $k_{total} = (k_1 + k_4) \times 2 + (k_2 + k_3) \times 4$, i.e., about 4.80×10^{-20} cm³/(mole·sec), which is close to the experiment value (5×10^{-20} cm³/(mole·sec)) of the reaction of PCDD/Fs with O_3, and the difference between rate constants may be attributed to the number of Cl atoms. It seems that the RRKM rate constants are reasonable.

Apart from the height of potential barriers, the rate constants are influenced significantly by the change of

Table 1 Rate constants of the elementary reaction of 2,3,7,8-TCDD with O_3 (unit: cm³/(mole·sec))

T (K)	R+O_3→TSa1→IMa1[a]	R+O_3→TSb1→IMb1[b]	R+O_3→TSc1→IMc1[c]	R+O_3→TSd1→IMd1[d]	2,3,7,8-TCDD+O_3→TS→IM[e]
200	1.90E-24	4.77E-24	2.09E-26	5.86E-27	2.30E-23
250	2.30E-22	4.40E-22	7.59E-24	2.40E-24	2.26E-21
298.15	5.66E-21	8.73E-21	3.76E-22	1.30E-22	4.80E-20
300	6.29E-21	9.70E-21	4.32E-22	1.49E-22	5.34E-20
350	7.29E-20	9.39E-20	8.43E-21	3.11E-21	5.61E-19
400	4.90E-19	5.41E-19	8.37E-20	3.25E-20	3.54E-18
450	2.27E-18	2.20E-18	5.27E-19	2.13E-19	1.59E-17
500	8.11E-18	6.96E-18	2.40E-18	1.01E-18	5.56E-17
550	2.38E-17	1.84E-17	8.59E-18	3.72E-18	1.63E-16
600	6.00E-17	4.22E-17	2.57E-17	1.14E-17	4.14E-16

[a] $k(T) = 2.49 \times 10^{-13} \exp(-5188.93/T)$; [b] $k(T) = 1.00 \times 10^{-13} \exp(-4803.81/T)$; [c] $k(T) = 6.62 \times 10^{-13} \exp(-6286.89/T)$; [d] $k(T) = 3.66 \times 10^{-13} \exp(-6425.55/T)$; [e] $k(T) = 2.41 \times 10^{-12} \exp(-5014.17/T)$.

temperature. Evidently, the rate constants of path A and path B are larger than those of path C and path D in low temperature range. While the rate constants of path C are larger than those of path A, path B and path D in high temperature range. The branching ratios of the four paths are drawn in **Fig. 6**. The branching ratio of path A increase gradually with the temperature rising. The proportion of path A varies from 17% to 29% in the range of 200–600 K. The branching ratio of path B decreases gradually as the temperature rises, which takes up the largest proportion (83%) in 200 K and the smallest proportion (41%) in 600 K. The branching ratios of path C and path D increase gradually with the temperature rising and that of path C takes the largest proportion (25%) at 600 K. It can be seen that the different paths play different roles at different temperatures, and the different paths will lead to a different degradation mechanisms.

In order to further consider the role of NO, H_2O and O_3 on the criegee intermediates, the rate constants of IMa2 with NO, H_2O and O_3 are calculated. The values are listed in the **Table 2**, which can provide a reference for experimental data. For the above dimolecular reaction, the reaction velocity (v) is

$$v = k[IMa2][X] \qquad X = NO, H_2O \text{ or } O_3 \qquad (9)$$

Since the concentration of X can be taken as a constant in the troposphere, the dimolecular reactions approximate the first order reactions. Then the roles of NO, H_2O or O_3 are changed vary with their concentrations in atmosphere.

The calculated rate constants for the reactions are expressed in the Arrhenius form of $k = A\exp(-E_a/RT)$ (in cm^3/(mole·sec)). The formula is given in **Tables 1** and **2**.

According to the rate constants of elementary reaction, the atmospheric lifetime of the reactants can be calculated (Sun et al., 2011). The lifetimes of the 2,3,7,8-TCDD and IMa2 over the range of 200–600 K are listed in **Table 3**. The lifetimes of reactants are helpful in the risk assessment of hazardous materials.

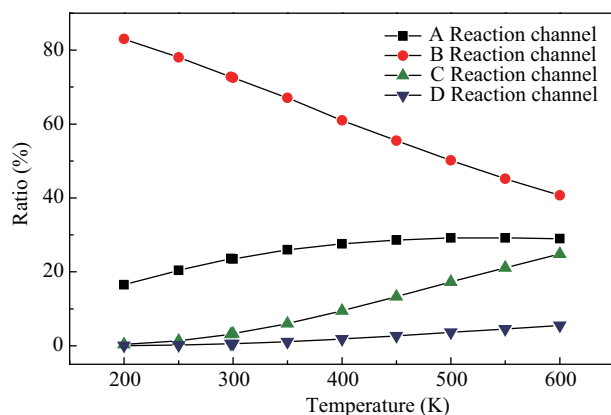The lifetime of 2,3,7,8-TCDD relative to O_3 is 11.50

Table 2 Rate constants of IMa2 react with O_3, H_2O and NO (unit: cm^3/(mole·sec))

T (K)	IMa2+O_3[a]	IMa2+H_2O[b]	IMa2+ NO[c]
200	1.94E-24	1.48E-19	7.82E-24
250	1.32E-22	1.01E-18	1.32E-21
298.15	2.15E-21	3.50E-18	3.92E-20
300	2.38E-21	3.66E-18	4.42E-20
350	1.98E-20	9.36E-18	5.83E-19
400	1.02E-19	1.93E-17	4.25E-18
450	3.08E-19	3.47E-17	2.07E-17
500	1.12E-18	5.65E-17	7.59E-17
550	2.80E-18	8.57E-17	2.25E-16
600	6.13E-18	1.23E-16	5.69E-16

[a] $k(T) = 8.20 \times 10^{-15}\exp(-4480.31/T)$; [b] $k(T) = 3.14 \times 10^{-15}\exp(-2010.89/T)$; [c] $k(T) = 3.88 \times 10^{-12}\exp(-5440.59/T)$.

Table 3 Lifetimes of 2,3,7,8-TCDD and IMa2 in atmosphere according to the rate constant at 200–600 K (unit: sec)

T (K)	2,3,7,8-TCDD	IMa2[a]	IMa2[b]	IMa2[c]
200	6.22E+10	7.36E+11	1.26E+01	4.76E+12
250	6.33E+08	1.08E+10	1.84E+00	2.82E+10
298.15	2.98E+07	6.64E+08	5.32E-01	9.49E+08
300	2.67E+07	6.00E+08	5.08E-01	8.42E+08
350	2.54E+06	7.22E+07	1.99E-01	6.38E+07
400	4.03E+05	1.40E+07	9.64E-02	8.76E+06
450	9.00E+04	4.64E+06	5.36E-02	1.80E+06
500	2.57E+04	1.28E+06	3.29E-02	4.90E+05
550	8.76E+03	5.10E+05	2.17E-02	1.65E+05
600	3.45E+03	2.33E+05	1.51E-02	6.54E+04

[a] O_3 average concentration is about 7×10^{11} mole/cm^3; [b] water average concentration is about 5.375×10^{17} mole/cm^3; [c] NO average concentration is about 2.6875×10^{10} mole/cm^3.

months at 298.15 K. The lifetimes of IMa2 relative to O_3, H_2O and NO are 21.05 years, 0.53 seconds and 30.09 years, respectively. Obviously, the water in atmosphere may play an important role in the degradation of IMa2.

The dioxins, including 2,3,7,8-TCDD, are distributed all over the atmosphere, such as gas phase, liquid phase, and the surface of gas-solid phase. The degradation mechanism in different phases should be further studied.

Fig. 6 Branching ratio of four reaction pathway at 200–600 K.

3 Conclusions

The ozonolysis mechanism of 2,3,7,8-TCDD is studied using the method of quantum chemistry calculation. The role of abundant precursors such as NO and H_2O in the atmosphere was also discussed. The rate constants were calculated using the RRKM theory at 200–600 K and the atmospheric lifetimes are estimated. The present study leads us to draw the following conclusions: (1) There are

existences of four reaction channels, any of which can take place. The potential barriers of four intramolecular reaction sites in 2,3,7,8-TCDD with the O_3 show that path A and path B are lower than those of path C and path D. (2) In the ozonolysis mechanism, the water is the source of the OH radical, which can initiate the subsequent degradation. (3) The total rate constant of 2,3,7,8-TCDD with O_3 is 4.80 $\times 10^{-20}$ cm^3/(mole·sec) and the lifetime is 11.50 months.

Acknowledgments

Supporting materials

Supplementary data associated with this article can be found in the online version.

R E F E R E N C E S

Al-Alawi S M, Abdul-Wahab S A, Bakheit C S, 2008. Combining principal component regression and artificial neural networks for more accurate predictions of ground-level ozone. *Environmental Modelling and Software*, 23(4): 396–403.

Altarawneh M, Dlugogorski B Z, Kennedy E M, Mackie J C, 2007. Quantum chemical investigation of formation of polychlorodibenzo-p-dioxins and dibenzofurans from oxidation and pyrolysis of 2-chlorophenol. *The Journal of Physical Chemistry A*, 111(13): 2563–2573.

Altarawneh M, Dlugogorski B Z, Kennedy E M, Mackie J C, 2008. Quantum chemical and kinetic study of formation of 2-chlorophenoxy radical from 2-chlorophenol: Unimolecular decomposition and bimolecular reactions with H, OH, Cl, and O_2. *The Journal of Physical Chemistry A*, 112(16): 3680–3692.

Atkinson R, 1996. Atmospheric chemistry of PCBs, PCDDs and PCDFs. *Environmental Science Technology*, 6: 53–72.

Chi K H, Chang M B, Kao S J, 2007. Historical trends of PCDD/Fs and dioxin-like PCBs in sediments buried in a reservoir in Northern Taiwan. *Chemosphere*, 68(9): 1733–1740.

Chi K H, Liu K T, Chang S H, Chang M B, 2009. Atmospheric deposition of PCDD/Fs measured via automated and traditional samplers in Northern Taiwan. *Chemosphere*, 77(9): 1184–1190.

Chiu J C, Shen Y H, Li H W, Lin L F, Wang L C, Chang-Chien G P, 2011. Emissions of polychlorinated dibenzo-p-dioxins and dibenzofurans from an electric arc furnace, secondary aluminum smelter, crematory and joss paper incinerators. *Aerosol and Air Quality Research*, 11(1): 13–20.

Choi J, Choi W, Mhin B J, 2004. Solvent-specific photolytic behavior of

octachlorodibenzo-p-dioxin. *Environmental Science and Technology*, 38(7): 2082–2088.

Choi W, Hong S J, Chang Y S, Cho Y, 2000. Photocatalytic degradation of polychlorinated dibenzo-p-dioxins on TiO$_2$ film under UV or solar light irradiation. *Environmental Science and Technology*, 34(22): 4810–4815.

Debecker D P, Delaigle R, Hung P C, Buekens A, Gaigneaux, E M, Chang M B, 2011. Evaluation of PCDD/F oxidation catalysts: Confronting studies on model molecules with tests on PCDD/F-containing gas stream. *Chemosphere*, 82(9): 1337–1342.

Fabian W M F, Janoschek R, 2006. Thermochemical properties of stable intermediates and derived radicals for the gas-phase formation of 1,3,6,8-and 1,3,7,9-tetrachlorodibenzo-p-dioxins from 2,4,6-trichlorophenol: A computational G3MP2B3 study. *Combustion and Flame*, 145(1-2): 282–289.

Fennell D E, Nijenhuis I, Wilson S F, Zinder S H, Hggblom M M, 2004. Dehalococcoides ethenogenes strain 195 reductively dechlorinates diverse chlorinated aromatic pollutants. *Environmental Science and Technology*, 38(7): 2075–2081.

Frisch M J, Trucks G W, Schlegel H B, Pople J A, 2003. Gaussian 03, Revision B. 03. Gaussian, Inc., Pittsburgh PA.

Hasson A S, Chung M Y, Kuwata K T, Converse A D, Krohn D, Paulson S E, 2003. Reaction of criegee intermediates with water vapors an additional source of OH radicals in alkene ozonolysis. *The Journal of Physical Chemistry A*, 107(32): 6176–6182.

Hilarides R J, Gray K A, Guzzetta J, Cortellucci N, Sommer C, 1994. Radiolytic degradation of 2,3,7,8-TCDD in artificially contaminated soils. *Environmental Science and Technology*, 28(13): 2249–2258.

Hou H, Wang B S, 2007. Ab initio study of the reaction of propionyl (C$_2$H$_5$CO) radical with oxygen (O$_2$). *The Journal of Physical Chemistry A*, 127(5): 054306.

Ide Y, Kashiwabara K, Okada S, Mori T, Hara M, 1996. Cataytic decomposition of dioxin from MSW incinerator flue gas. *Chemosphere*, 32(1): 189–198.

José R S, Stohl A, Karatzas K, Bohler T, James P, Pérez J L, 2005. A modelling study of an extraordinary night time ozone episode over Madrid domain. *Environmental Modelling and Software*, 20(5): 587–593.

Khachatryan L, Burcat A, Dellinger B, 2003. An elementary reaction-kinetic model for the gas-phase formation of 1,3,6,8- and 1,3,7,9-tetrachlorinated dibenzo-p-dioxins from 2,4,6-trichlorophenol. *Combustion and Flame*, 132(3): 406–421.

Konstantinov A D, Johnston A M, Cox B J, Petrulis J R, Orzechowski M T, Bunce N J et al., 2000. Photolytic method for destruction of dioxins in liquid laboratory waste and identification of the photoproducts from 2,3,7,8-TCDD. *Environmental Science and Technology*, 34(1): 143–148.

Kulkarni P S, Crespo J G, Afonso C A M, 2008. Dioxins sources and current remediation technologies – A review. *Environment International*, 34(1): 139–153.

Kwok E S C, Atkinson R, 1995. Estimation of hydroxyl radical reaction-rate constants for gas-phase organic-compounds using a structure-reactivity relationship: an update. *Atmospheric Environment*, 29(14): 1685–1695.

León L A, Notario R, Quijano J, Sánxhez C, 2002. Structures and enthalpies of formation in the gas phase of the most toxic polychlorinated dibenzo-p-dioxins: A DFT Study. *The Journal of Physical Chemistry A*, 106(28): 6618–6627.

Lin L F, Lee W J, Chang-Chien G P, 2008. Emissions of polychlorinated dibenzo-p-dioxins and dibenzofurans from various industrial sources. *Journal of Air Waste Management Association*, 56(12): 1705–1715.

Lundin L, Marklund S, 2005. Thermal degradation of PCDD/F in municipal solid waste ashes in sealed glass ampules. *Environmental Science and Technology*, 39(10): 3872–3877.

Mori T, Kondo R, 2002. Oxidation of chlorinated dibenzo-p-dioxin and dibenzofuran by white-rot fungus, Phlebia lindtneri. *FEMS Microbiology Letters*, 216(2): 223–227.

Qu X H, Wang H, Zhang Q Z, Shi X Y, Xu F, Wang W X, 2009. Mechanistic and kinetic studies on the homogeneous gas-phase formation of PCDD/Fs from 2,4,5-trichlorophenol. *Environmental Science and Technology*, 43(11): 4068–4075.

Rayne S, Wan P, Ikonomou M J, Konsstantinov A D, 2002. Photochemical mass balance of 2,3,7,8-TeCDD in aqueous solution under UV light shows formation of chlorinated dihydroxybiphenyls, phenoxyphenols, and dechlorination products. *Environmental Science and Technology*, 36(9): 1995–2002.

Schecter A, 1994. Dioxin and Health. Plenum Press, New York.

Schecter A, Bimbaum L, Ryan J J, Constable J D, 2006. Dioxins: An overview. *Environmental Research*, 101(3): 419–428.

Sun X M, Bai J, Zhao Y Y, Zhang C X, Wang Y D, Hu J T, 2011. Chemical mechanism and kinetics study on the Ocimene Ozonolysis reaction in atmosphere. *Atmospheric Environment*, 45(34): 6197–6203.

Sun T L, Wang Y D, Zhang C X, Sun X M, Wang W X, 2011. The chemical mechanism of the limonene Ozonolysis reaction in the SOA formation: A quantum chemistry and direct dynamic study. *Atmospheric Environment*, 45(9): 1725–1731.

Vollmuth S, Niessner R, 1995. Degradation of PCDD, PCDF, PAH, PCB and chlorinated phenols during the destruction-treatment of landfill seepage water in laboratory model reactor (UV, ozone, and UV/ozone). *Chemosphere*, 30(12): 2317–2331.

Wang F, Sun H, Sun J Y, Jia X J, Zhang Y J, Tang Y Z et al. 2010. Mechanistic and kinetic study of CH_2O+O_3 reaction. *The Journal of Physical Chemistry A*, 114(10): 3516–3522.

Weber R, Sakurai T, Hagenmaier H, 1999. Formation and destruction of PCDD/Fs during heat treat treatment of fly ash samples from fluidized bed incinerators. *Chemosphere*, 38(11): 2633–2642.

Wen Z C, Wang Z H, Xu J R, Zhou J H, Cen K F, 2010. Quantum chemistry study on the mechanism of the reaction between Ozone and 2,3,7,8-TCDD. *International Journal of Quantum Chemistry*, 111(5): 1081–1091.

Xu F, Wang H, Zhang Q Z, Zhang R X, Qu X H, Wang W X, 2010. Kinetic properties for the complete series reactions of chlorophenols with OH radicals-relevance for dioxin formation. *Environmental Science and Technology*, 44(4): 1399–1404.

Xu F, Yu W N, Gao R, Zhou Q, Zhang Q Z, Wang W X, 2010. Dioxin formations from the radical/radical cross-condensation of Phenoxy radicals with 2-chlorophenoxy radicals and 2,4,6-trichlorophenoxy radicals. *Environmental Science and Technology*, 44(17): 6745–6751.

Xu F, Yu W N, Zhou Q, Gao R, Sun X Y, Zhang Q Z et al., 2011. Mechanism and direct kinetic study of the polychlorinated dibenzo-p-dioxin and dibenzofuran formations from the radical/radical cross-condensation of 2,4-dichlorophenoxy with 2-chlorophenoxy and 2,4,6-trichlorophenoxy. *Environmental Science and Technology*, 45(2): 643–650.

Yang J, Li Q S, Zhang S W, 2007. Reaction-path dynamics and theoretical rate constants for the reaction $CH_4+O_3 \rightarrow HOOO+CH_3$. *International Journal of Quantum Chemistry*, 107(10): 1999–2005.

Yang J, Li Q S, Zhang S W, 2008. Direct dynamics study on the reaction of acetaldehyde with ozone. *Journal of Computational Chemistry*, 29(2): 247–255.

Yu W N, Hu J T, Xu F, Sun X Y, Gao R, Zhang Q Z et al., 2011. Mechanism and direct kinetics study on the homogeneous gas-phase formation of PBDD/Fs from 2-BP, 2,4-DBP, and 2,4,6-TBP as precursors. *Environmental Science and Technology*, 45(5): 1917–1925.

Zhang C X, Sun T L, Sun X M, 2011. Mechanism for OH-initiated degradation of 2,3,7,8-tetrachlorinated dibenzo-p-dioxins in the presence of O_2 and NO/H_2O. *Environmental Science and Technology*, 45(11): 4756–4762.

Zhang C X, Zhao Y Y, Bai J, Gong C, Sun X M, 2012. Mechanism and kinetic study on the OH-initiated degradation of 2,3,7,8-tetrachlorinated dibenzofuran in atmosphere. *Science of the Total Environment*, 435-436: 53–60.

Zhang Q Z, Li S Q, Qu X H, Shi X Y, Wang W X, 2008. A quantum mechanical study on the formation of PCDD/Fs from 2-chlorophenol as precursor. *Environmental Science and Technology*, 42(19): 7301–7308.

Zhang Q Z, Yu W N, Zhang R X, Zhou Q, Gao R, Wang W X, 2010. Quantum chemical and kinetic study on dioxin formation from the 2,4,6-TCP and 2,4-DCP precursors. *Environmental Science and Technology*, 44(9): 3395–3403.

Zhang R Q, Huang J H, Bu Y X, Han K L, Lee S T, He G Z, 2000. An effective scheme for selecting basis sets for ab initio calculations. *Science in China (Series B)*, 43(4): 375–388.

Zhao Y, Truhlar D G, 2004. Hybrid meta density functional theory methods for thermochemistry, thermochemical kinetics, and non-covalent interactions: The MPW1B95 and MPWB1K models and comparative assessments for hydrogen bonding and van der Waals interactions. *Journal of Physical Chemistry A*, 108(33): 6908–6908.

Editorial Board of Journal of Environmental Sciences

JOURNAL OF ENVIRONMENTAL SCIENCES

环境科学学报(英文版)

(http://www.jesc.ac.cn)